JOURNAL OF VIROLOGY, Aug. 1976, p. 501-517

Vol. 19, No. 2
Printed in U.S.A.

Analysis of Gene Function of Bacteriophage ϕ29 of *Bacillus subtilis*: Identification of Cistrons Essential for Viral Assembly

ELAINE W. HAGEN, BERNARD E. REILLY, MARIO E. TOSI, AND DWIGHT L. ANDERSON*
Department of Microbiology and School of Dentistry, University of Minnesota, Minneapolis, Minnesota 55455

Received for publication 13 February 1976

Restrictive infection of *Bacillus subtilis* by suppressor-sensitive (*sus*) mutants of ϕ29 has been used to search for cistrons that function in viral assembly. The products of cistrons 7, 9, 10, and 16 are necessary for head morphogenesis. The neck upper collar protein P10 and the tail protein P9 must be present for DNA packaging to occur. The protein P7 must be present for phage-related particles to form. A prohead-like particle has been isolated during 16^- restrictive infection. The particle is composed of the proteins Hd, P10, F, and P7. P16 must function for DNA-filled particles to accumulate. A DNA-containing particle produced in the absence of the cistron 11 product may be an intermediate in the ϕ29 assembly pathway. The protein P13 interacts with P9 and P11 to form a stable DNA-filled particle. The products of cistrons 2 and 3 are essential for viral DNA synthesis, and in their absence virus-related particles are not detected.

The *Bacillus subtilis* phage ϕ29 has a complex morphology, and seven viral structural proteins resolved by electrophoresis have been identified as components of the head, neck, and tail (1, 14).

The genome of ϕ29 is a DNA duplex with a molecular weight of about 11×10^6, and in the virion the ends of the DNA molecule are linked by a specific protein (1, 17). Reference mutants from the Madrid (15) and Minneapolis collections (20, 21) have been used to construct a linear genetic map consisting of 17 cistrons in an unambiguous order (13). At least 23 viral-induced proteins have been resolved in lysates of UV-irradiated *B. subtilis* by sodium dodecyl sulfate (SDS)-polyacrylamide gel electrophoresis and autoradiography (4, 7, 12, 18).

We began our study of ϕ29 morphogenesis by examining cleavage and assembly of the neck appendage protein. The product of cistron 12, the protein P12, is cleaved to generate the neck appendage protein (Ap) and a low-molecular-weight protein (LM2) (2, 7). This observation has been confirmed by pulse-chase experiments and by comparison of tryptic digests of proteins P12 and Ap (3, 25). Each of the 12 appendages consists of a single protein molecule that is attached to the lower of two collars. These structures define the neck of the virus. The appendages contain the main serum blocking power of ϕ29 and are in close contact with the cell wall during adsorption (24). The proteolytic processing of the protein P12 does not require interaction with the maturing neck structure, and the cleaved appendages are biologically active in an in vitro complementation system (25).

In this communication we have examined restrictive infection by suppressor-sensitive (*sus*) reference mutants to identify viral-induced proteins that play a role in ϕ29 assembly. We have measured viral DNA synthesis, identified structures by both the thin sectioning and the in situ lysis techniques of electron microscopy, and isolated particles whenever possible by sucrose gradient centrifugation. The protein composition of the purified particles has been determined by SDS-polyacrylamide gel electrophoresis and autoradiography.

MATERIALS AND METHODS

Chemicals and isotopes. The serylprotease inhibitor phenylmethylsulfonylfluoride (Sigma Chemical Co., St. Louis, Mo.) was dissolved in 95% ethanol to give a stock solution of 6 mg/ml and used at a final concentration of 300 μg/ml. Egg white lysozyme (A grade), DNase I (B grade), and RNase (bovine pancreatic) were from Calbiochem.

The ^{14}C-labeled amino acid mixture (New England Nuclear Corp., NEC-445; 100 μCi/ml, about 200 mCi/mmol) was adjusted to neutrality by the addition of a 0.1 volume of 1 N NaOH immediately before use. [^{3}H]thymidine was from New England Nuclear Corp. (NET-027Z; 1 mCi/ml, 50 Ci/mmol).

Phage and bacteria. Phage ϕ29 (19) was employed. The ϕ29 *sus* mutants were isolated after mutagenesis with hydroxylamine (21) or bromodeoxyuridine (20). Mutants constructed by recombina-

tion with *sus*14(1241) (25) have a delayed lysis phenotype. The mutants *sus*14(1241), *sus*15(212), and *sus*17(112) were isolated in Madrid (15).

The properties of *B. subtilis* SpoA12 and *B. subtilis* L15, the nonpermissive and permissive bacterial hosts, respectively, have been described (21).

Media. Minimal medium M40 (25) supplemented with 50 μg of tryptophan per ml (M40t medium) was employed for phage infections, except for the in situ lysis experiments, in which antibiotic medium 3 (PB; Difco) was used. The phage stocks were maintained in TMS buffer (25) or in antibiotic medium 3.

Growth conditions, UV irradiation, and infection. Protocols described previously (7, 25) were generally followed. Bacteria were grown to 2 × 10^8 cells/ml, concentrated to 2 × 10^9 cells/ml by centrifugation, UV irradiated (50 ergs/mm^2 per s) in M40t when indicated, infected with a multiplicity of infection (MOI) of 20 or 50, and then diluted to 2 × 10^8 cells/ml with prewarmed (37°C) M40t medium after adsorption for 2.5 or 5 min. The MOI as well as the time and temperature of adsorption are specified below for each type of experiment. The M40t medium was sometimes supplemented with 100 or 200 μg of Casamino Acids (Difco) per ml (M40ta medium).

Analysis of viral DNA synthesis. Bacteria grown in M40ta medium and concentrated to 2 × 10^9/ml were treated for 5 min at 37°C with 200 μg of 6-(*p*-hydroxyphenylazo)uracil per ml as described previously (23) and then infected with phage at an MOI of 50 (0 time). At 2.5 min after infection, the cells were diluted 10-fold with M40ta medium containing [^{3}H]thymidine (50 μCi/ml), HPUra (200 μg/ml), and deoxyguanosine (500 μg/ml; to promote thymidine incorporation) and incubated at 37°C with shaking. Culture samples (100 μl) were removed at intervals after infection, and the incorporation of [^{3}H]thymidine into trichloroacetic acid-insoluble material was measured as described previously (23).

Radioactive labeling of proteins. UV-irradiated cells at 2 × 10^9/ml in M40t medium at 37°C were infected with phage at an MOI of 50 (0 time). For labeling of early proteins, the culture was diluted to 2 × 10^8 cells/ml with prewarmed M40t medium containing ^{14}C-labeled amino acids (10 μCi/ml) at 2 min after infection, and labeling was terminated at 8 min as described previously (7). Early and late proteins were continuously labeled with ^{14}C-amino acids (4 μCi/ml) from 2.5 to 45 min.

Isolation of viral structures. Cells grown in M40ta medium were infected at an MOI of 20. After a 5-min adsorption period at 22°C, the infected cells were collected on membrane filters (pore size, 0.45 μm; Millipore Corp.), washed with M40ta medium to remove unadsorbed phage, suspended in prewarmed (37°C) M40ta medium containing the ^{14}C-labeled amino acid mixture (10 μCi/ml), and incubated at 37°C with shaking until 100 to 120 min after infection. After terminating labeling (7), cells were collected by centrifugation and suspended in a volume of TMS $^1/_{50}$ that of the original culture; the concentrated cells were lysed and processed for sucrose gradient analysis as described previously (25). Samples were centrifuged in gradients of 5 to 20% sucrose in TMS buffer in an SW50.1 rotor at 35,000 rpm for 29 min at 23°C. The gradients were formed and fractionated as described previously (25).

Electron microscopy. In situ experiments with φ29 *sus* mutants were performed using methods described previously (6). To observe viral structures in thin sections, bacteria concentrated to 2 × 10^9/ml were infected at an MOI of 10. At 10 min after infection, the cells were diluted 10-fold into prewarmed PB and incubated for an additional 45 min. Infected cells from 2 ml of culture were sedimented

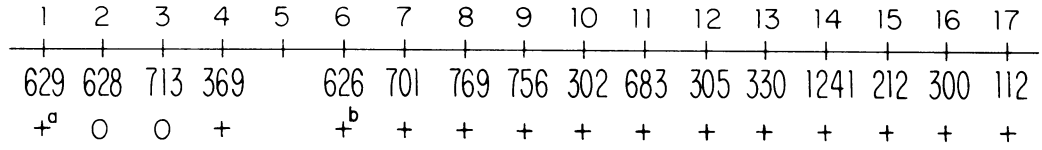

FIG. 1. *Genetic map of φ29 that merely reflects cistron order. Recombination frequencies are not implied. Cistron numerals appear above the line; the reference mutants used appear below. (a) Viral DNA synthesis was measured during sus mutant infection of the nonpermissive host B. subtilis SpoA12 as described in Materials and Methods; the range of DNA synthesis indicated by + is illustrated in Fig. 3. (b) Viral DNA synthesis is delayed (see Fig. 3).*

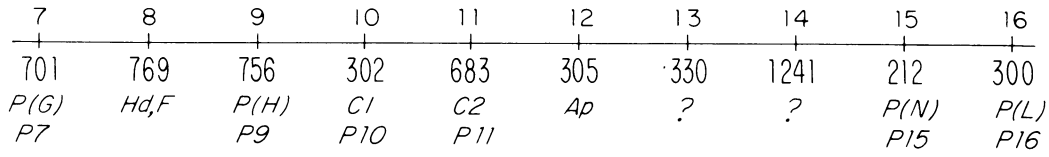

FIG. 2. *A portion of the genetic map of φ29. Recombination frequencies are not implied, merely cistron order. Cistron numerals appear above the line; reference mutants used appear below. The next series of symbols refers to viral proteins described previously (7), and below we give our new convention for naming the cistron products. P(G), Low-molecular-weight protein LM5B; Hd, major head protein; F, head fiber; P(H), tail protein; C1, neck upper collar protein; C2, neck lower collar protein; Ap, neck appendage.*

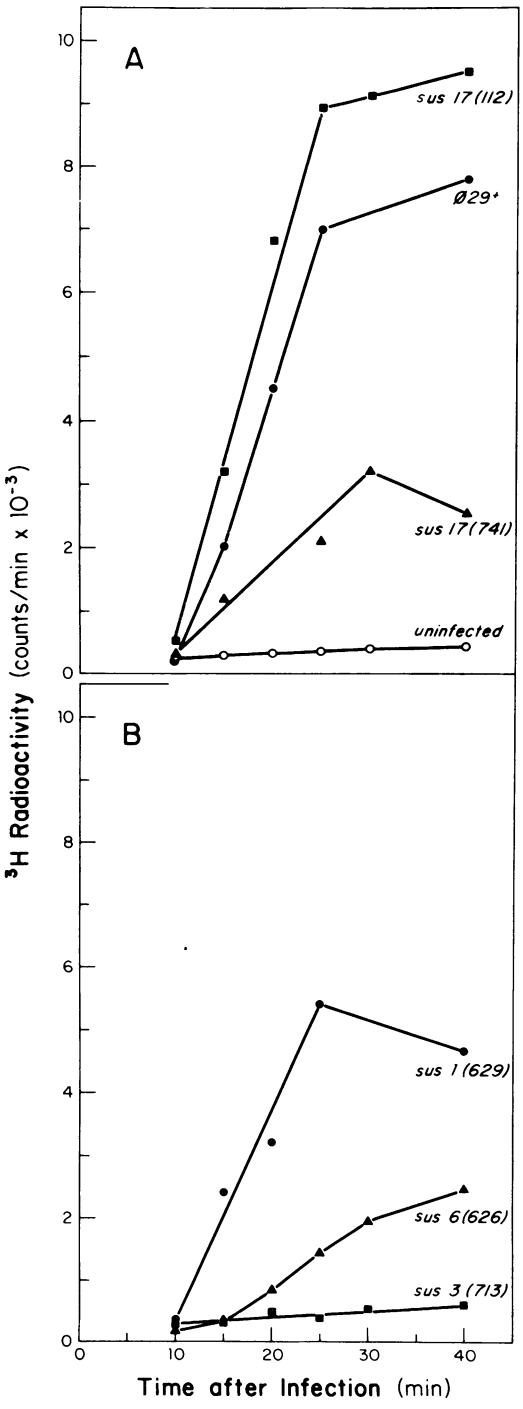

FIG. 3. *Incorporation of [³H]thymidine into viral DNA in the nonpermissive host infected with sus mutants or wild-type φ29.*

and fixed by suspending the pellet in 1 ml of 3.3% buffered glutaraldehyde prepared by diluting 70% glutaraldehyde (Ladd Research Industries, Burlington, Vt.) in Palade buffer containing 0.028 M sodium acetate and 0.028 M sodium barbital, pH 7.3. After 18 to 24 h, cells were sedimented and postfixed for 4 h at 4°C with osmium by suspending the pellet in a mixture of 2.5 ml each of Kellenberger fixative and tryptone medium (9). After a standard dehydration procedure (9), the fixed cells were embedded in Epon 812 (4A:6B) epoxy resin (11). Thin sections on carbon-coated Formvar films were stained with lead citrate (22). Phage structures from peak fractions of sucrose gradients were fixed for microscopy by adding glutaraldehyde (8%, Polysciences, Warrington, Pa.) to a final concentration of 0.4%. Carbon-reinforced Formvar-coated grids were floated over the sample drops for 5 to 10 min and then transferred successively through single drops of 10% sucrose in TMS, 5% sucrose in TMS, and neutral 1.5% (wt/vol) sodium phosphotungstate to negatively stain. Micrographs were taken with a Philips EM301 electron microscope at 80 kV.

Electrophoresis. Proteins were separated by SDS-gel electrophoresis as described previously (2), except for the following modification. Linear polyacrylamide gradients of 12 to 19% were formed in an SE520-.75 slab gel device (Hoefer Scientific, San Francisco, Calif.). The gels were 29 cm in length and 0.75 mm in thickness and contained a 12 to 19% gradient of glycerol in parallel with the polyacrylamide. The gels were polymerized for 12 h at 10°C and run at 10°C. Stacking was at 50 V (constant voltage), and separation was at 10 W (constant power). Gels were successively fixed in 45% methanol-10% acetic acid and 30% methanol-10% acetic acid prior to drying. The dried gels were processed for autoradiography as described previously (2).

Protein composition of φ29-related structures. ^{14}C-labeled proteins in φ29-related structures isolated by sucrose gradient centrifugation were separated by electrophoresis as described above. Protein bands were cut from dried gels and analyzed for radioactivity after combustion in a Packard Tri-Carb oxidizer (model 306) as described previously (25).

RESULTS

The reference φ29 mutants of the Madrid (15) and Minneapolis (20, 21) collections have been used to construct a linear genetic map. Three-factor crosses have been used to unambiguously order the 17 cistrons, and they have been numbered sequentially from left to right (cistrons 1–17) according to their relative position on the map (Fig. 1) (13). Figure 2 illustrates the changes in nomenclature accompanying the numbering of the φ29 cistrons, including cistrons known to specify structural proteins. The protein product of cistron *n* is referred to as P*n*. For example, the product of cistron 11, the neck lower collar protein, is named P11.

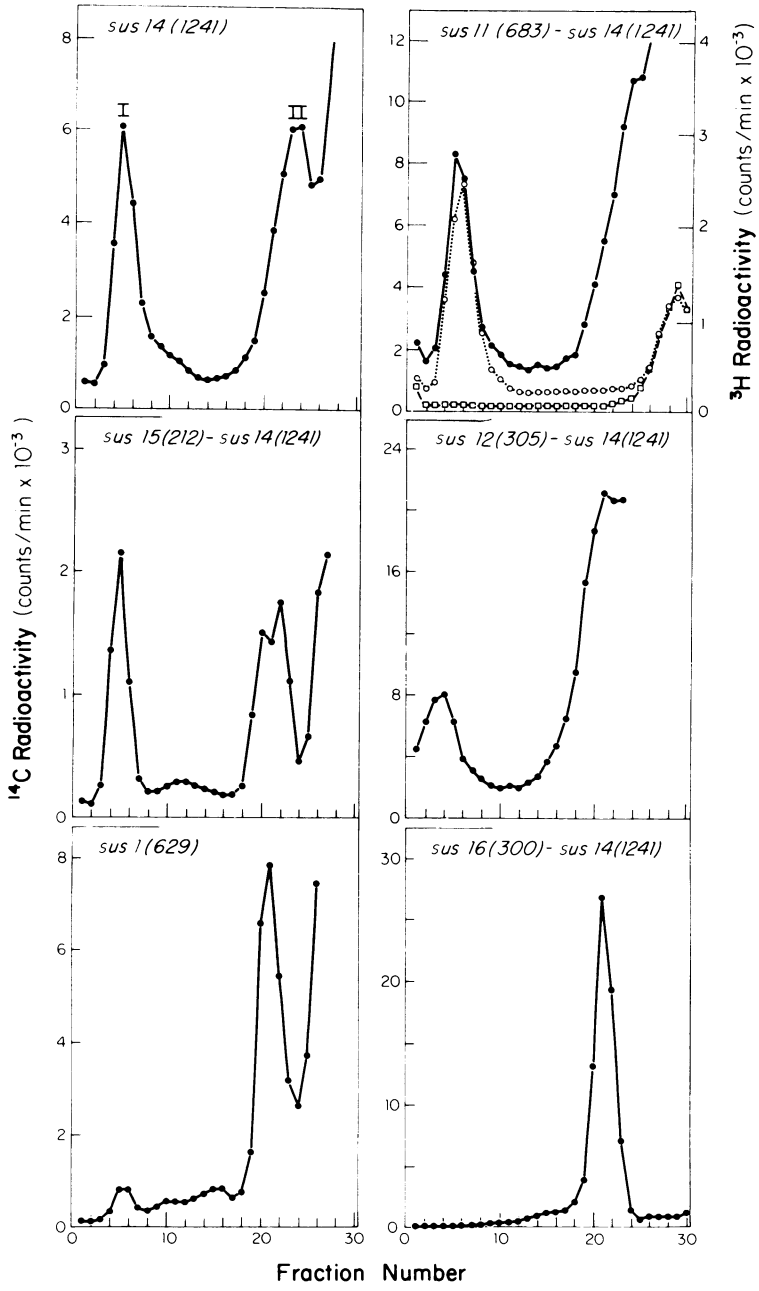

FIG. 4. *Sucrose gradient isolation of φ29-related structures containing ^{14}C-labeled protein (●) or [^{3}H]DNA (○) from lysates of sus mutant-infected B. subtilis SpoA12. [^{3}H]DNA in an uninfected culture is shown as a control (□). Conditions for preparation of lysates, centrifugation, and determination of radioactivity are as described. The ^{14}C-labeled peaks I and II are not present in an uninfected control, and peak I of the 14(1241)$^{-}$ lysate contains the bulk of the infectivity for the permissive host (25).*

Viral DNA synthesis in restrictive *sus* mutant infections. We have extended our examination of φ29 DNA synthesis in the presence of 6-(*p*-hydroxyphenylazo)uracil, an inhibitor of *B. subtilis* DNA synthesis (23). The incorporation of [^{3}H]thymidine into φ29 DNA in the presence of HPUra was followed during infection of the nonpermissive host *B. subtilis*

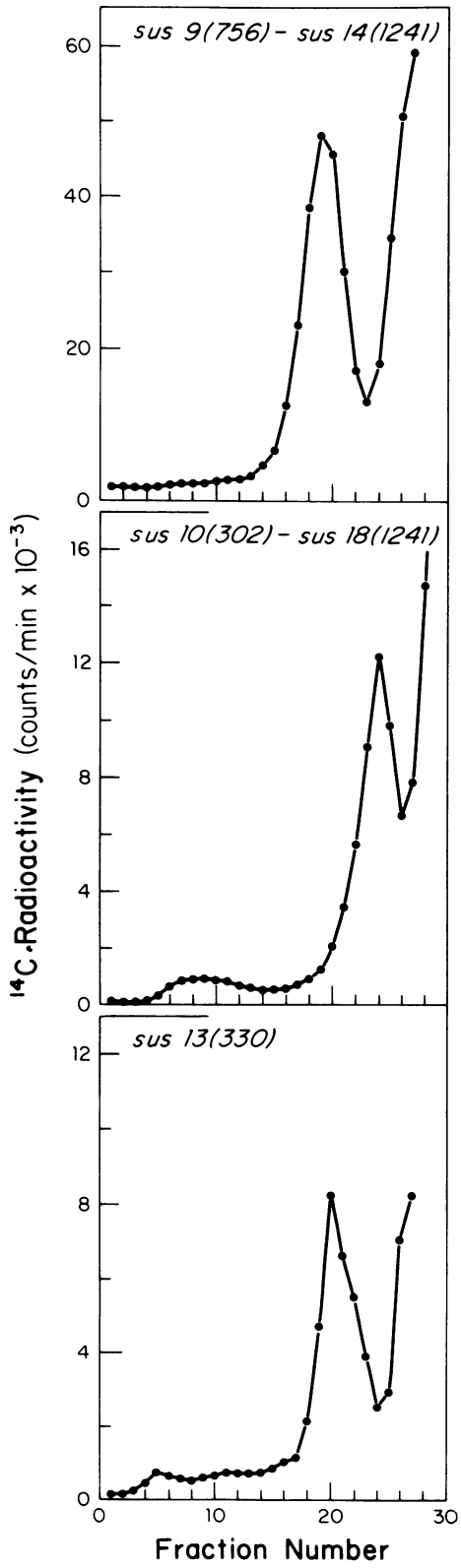

SpoA12 by reference *sus* mutants. The results are summarized in Fig. 1. The viral DNA synthesis observed after infection by mutant *sus*17(112) (Fig. 3A) was typical for results recorded as "+" in Fig. 1, with the possible exceptions of mutants *sus*1(629) and *sus*6(626) (Fig. 3B). The amount and kinetics of [^{3}H]thymidine incorporation depicted for these two mutant infections is typical and can be contrasted with the results obtained with mutant *sus*3(713) infection, in which DNA synthesis is not detected in the nonpermissive host. The results with mutant *sus*17(741) are included as a reminder that all mutants placed in a given cistron do not have identical phenotypes.

Isolation of phage-related structures. The isolation of head-related structures from lysates of *sus* mutant-infected nonpermissive cells in 5 to 20% sucrose gradients is illustrated in Fig. 4 and 5. Because the mutant *sus*14(1241) has a delayed lysis phenotype and an infected cell accumulates at least 500 infectious phage, this mutant has been used to construct recombinants with our reference mutants (15, 25). Infection with these recombinants, as illustrated in Fig. 4, generally results in the synthesis of large numbers of defective particles during the extended latent period. The peaks labeled I and II in the profile of mutant *sus*14(1241)-infected cells are typically observed when a lysate contains structures with and without DNA, respectively. As shown in Table 1, the peak I particles obtained after restrictive infection by mutant *sus*14(1241) (Fig. 4) have the protein composition expected of φ29; we have estimated the number of copies of the structural proteins of wild-type φ29 first by assuming 102 copies of the major head protein (M. Tosi, Ph.D. thesis, Univ. of Basel, Switzerland, 1975) and then using the value of 12 copies of the appendage protein (25). Cosedimentation of [^{3}H]thymidine label with peak I particles is illustrated with a lysate of *sus*11(683)-*sus*14(1241)-infected cells in Fig. 4.

Infection by mutants of cistrons 11, 12, 14 and 15 results in the production of DNA-containing particles sedimenting in peak I (Fig. 4). DNA-containing particles are rarely detected after infection by mutants of cistrons 9, 10, 13 and 16 (Fig. 4 and 5). Nonpermissive cells infected by *sus*1(629) frequently produce a small burst of phage (data not shown), and only a few DNA-

FIG. 5. *Sucrose gradient isolation of ^{14}C-labeled φ29-related structures from lysates of sus mutant-infected B. subtilis SpoA12. Conditions for preparation of lysates, centrifugation, and determination of radioactivity are as described in Materials and Methods.*

TABLE 1. *Copies of proteins in φ29 head-related structures*

sus mutant[a]	Protein[b]							
	Ap	P9	Hd	P10	P11	F	P15	P7
φ29+[c]	11.9	2.6	102	5.6	4.3	49		
φ29+[c]	12	2.6	103	5.7	4.3	49		
14(1241)I	13.3	2.5	102	5.4	4.9	50		
9(756)IIA	2.6		102	5.6	2.3	35	2.9	18
9(756)IIB	2.4		102	5.7	1.7	38	2.3	18
10(302)II			72[d]			38		29
16(300)IIA			102	5.1		25		40
16(300)IIB			102	4.9		25		42
11(683)I			102	4.9		51		
11(683)II			102	5.6		44		16
12(305)II			102	3.3		44		28

[a] I and II represent the fast- and slow-sedimenting particles, respectively, in peaks of sucrose gradients (Fig. 4 and 5). A and B represent results from two independent particle isolations.

[b] Radioactivity in each protein was determined by combusting gel fractions as described. Copies were determined from the reported molecular weights of φ29 proteins (7) by assuming 102 copies of the major head protein (Tosi, Ph.D. thesis, University of Basel, 1975), except as noted in footnote c below. ^{14}C radioactivity (counts per minute) in the major head protein in samples φ29+ through 12(305)II, respectively, was 4773, 4777, 1743, 3428, 3264, 1396, 2041, 2892, 823, 2536 and 1674.

[c] Using the average counts per minute of two determinations for each protein, copies were calculated relative to protein Hd (top row) or protein Ap (second row). Twelve copies of Ap are present in the mature virion (1, 25).

[d] Estimate based on a model for the isometric form of φ29 derived by removing equatorial subunits.

containing structures are present in the peak I position (Fig. 4).

Head-related particles were not observed after restrictive infection by mutants of cistrons 2, 3, 4, and 8 when the infected cells were examined by the thin sectioning or in situ lysis techniques of electron microscopy (micrographs not shown). DNA is not synthesized in the *sus*2(628) and *sus*3(713) restrictive infections (Fig. 1 and 3), although all of the late proteins are produced (2). In contrast, viral DNA is synthesized after infection of nonpermissive cells by the mutants *sus*4(369) and *sus*8(769) (Fig. 1); however, the major head protein is not produced (2) and head-related structures are absent.

Morphology and composition of 7⁻, 9⁻, and 10⁻ phage-related structures. The structures produced during restrictive infection by *sus* mutants of cistrons, 7, 9, and 10 may be abortive rather than true intermediates in φ29 assembly.

Mutants of cistron 7 are unable to synthesize protein P7 (Fig. 6f-i), a protein previously referred to as LM5B (7). Examination with the in situ lysis technique of nonpermissive cells infected by *sus*7(701) (Fig. 7) revealed fragile structures with a low degree of organization that tended to appear in clusters.

The particles produced during restrictive infection by the mutant *sus*9(756) (Fig. 8B) do not contain significant amounts of DNA and sediment in peak II (Fig. 5). In addition to the structural proteins Ap, Hd, P10, P11 and F, these particles contain the proteins P7 and P15 (Fig. 2 and 9b; Table 1). Reduced amounts of Ap, P11, and F are detected. When particles lack DNA but contain protein P7 we observe an electron-dense core (Fig. 8B).

Cistron 10 mutant infection yields particles with an isometric form (Fig. 8A) and an electron-dense core that sediment in peak II (Fig. 5). The proteins Hd, F, and P7 are present (Fig. 2 and 9f; Table 1). The neck upper collar protein, P10, is not synthesized (2), and the morphology of the 10⁻ particle suggests that P10 plays an essential role in the formation of the normal prolate head.

Morphology and composition of 11⁻, 12⁻, 13⁻, and 16⁻ particles. The particles produced during restrictive infection by *sus* mutants of cistrons 11, 12, 13, and 16 may all be true intermediates in the φ29 assembly pathway. The 12⁻ particles have been proven to be true intermediates by in vitro complementation (25).

During restrictive infection by cistron 16 *sus* mutants, in situ lysis reveals prolate heads without neck or tail that appear less angular than φ29 heads (Fig. 10). Thin sections of 16⁻-

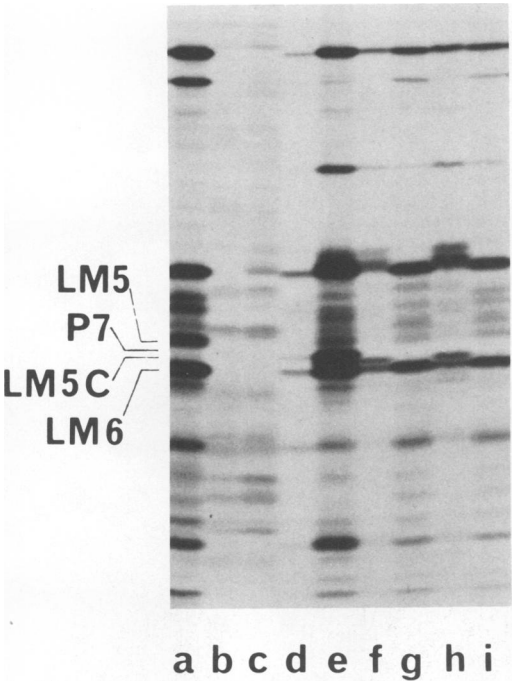

FIG. 6. *Autoradiographs of ^{14}C-labeled ϕ29-specific proteins produced in sus mutant and wild-type infections of UV-irradiated B. subtilis SpoA12. Cells were infected with a sus mutant or the wild type (MOI of 50) and labeled with a mixture of ^{14}C-amino acids from 2 to 8 min (a and b) or from 2.5 to 45 min (c–i). Cell and/or supernatant fractions were analyzed by SDS-gel electrophoresis as described in Materials and Methods. Profiles (e), (f), and (h) are of supernatants, and profiles (a), (b), (c), (d), (g), and (i) are of cell pellets. Profiles (b) and (c) are from uninfected control cultures; profiles (a), (d), and (e) are from ϕ29$^+$-infected cultures. Results of infection with sus7(614) are shown in (f) and (g), and profiles (h) and (i) are from infection with sus7(701).*

infected cells show clustered particles with indistinct boundaries (Fig. 11A). The 16$^-$ particles are found in peak II of the sucrose gradient (Fig. 4) and consist of the proteins Hd, P10, F, and P7 (Fig. 9c and Table 1). This particle has an electron-dense core and is less angular than the head of the virion (Fig. 12A). The head fibers are not readily visible by electron microscopy. The 16$^-$ particle is very similar in morphology and protein composition to an intermediate in ϕ29 assembly that we have termed the prohead (16).

Large numbers of seemingly normal prolate heads were observed by the in situ lysis technique after restrictive infection by mutant *sus*11(771) (Fig. 13). The absence of the neck lower collar protein P11 (2) results in an inability to assemble the neck or tail on the head. The cistron 11(683)$^-$ particles sediment in two peaks in the sucrose gradient (Fig. 4). The fast-sedimenting particles illustrated in Fig. 12B contain DNA and the proteins Hd, F, and P10 (Fig. 4 and 9d; Table 1). The 11$^-$ particles of peak II depicted in Fig. 12C are devoid of DNA (Fig. 4) and consist of a mixture of electron-dense prohead-like particles and "empty" particles that have angular profiles. The protein P7 is found in this peak (Fig. 9e; Table 1), a finding consistent with the presence of prohead-like particles.

Restrictive infection by *sus* mutants of cistron 12 also generates particles that sediment in peaks I and II (Fig. 4). The fast-sedimenting particles are morphologically complete except for the absence of the neck appendage protein (Fig. 12D), which can be added in vitro to produce infectious phage (25). Electrophoresis demonstrates that these particles contain P9, Hd, P10, P11, and F (data not shown). The 12$^-$ particles of peak II shown in Fig. 12E resemble the 16$^-$ particles (Fig. 12A) morphologically, lack DNA, and contain the proteins Hd, P10, F, and P7 (Fig. 9g; Table 1).

When nonpermissive cells infected with the *sus*13(330) mutant are observed by thin sectioning, most particles have the angularity and form of the viral head, and about two-thirds of them have the electron density characteristic of DNA-filled particles (Fig. 11B). The "empty" particles have a definite boundary that distinguishes them from the cistron 16$^-$ defective particles (Fig. 11A). The 13$^-$ particle that sediments in peak II (Fig. 5) of the sucrose gradient has apparently lost its DNA and contains the structural proteins Ap, Hd, P10, P11, and F (data not shown). Consistent with the absence of DNA, the protein P7 is present in barely detectable amounts in this particle (data not shown), and accordingly the majority of the particles do not have an electron-dense core (Fig. 8C). Most cistron 13(55)$^-$ particles have tails and in this respect differ from the 13(330)$^-$ particles (data not shown).

Restrictive *sus* mutant infections that yield a significant wild-type burst. The slow-sedimenting cistron 1$^-$ particles isolated by sucrose gradient centrifugation (Fig. 4) resemble the peak II particles of the 11$^-$, 12$^-$, and 16$^-$ infections in that they have electron-dense cores (Fig. 14). The protein composition of the 1$^-$ particle (data not shown) is identical to that of the 16$^-$ particle (Table 1).

Restrictive infection with the mutant *sus*15(212) yielded a burst size about 15% that of wild-type ϕ29, and the sucrose sedimentation profile of the cistron 15$^-$ particles resembles

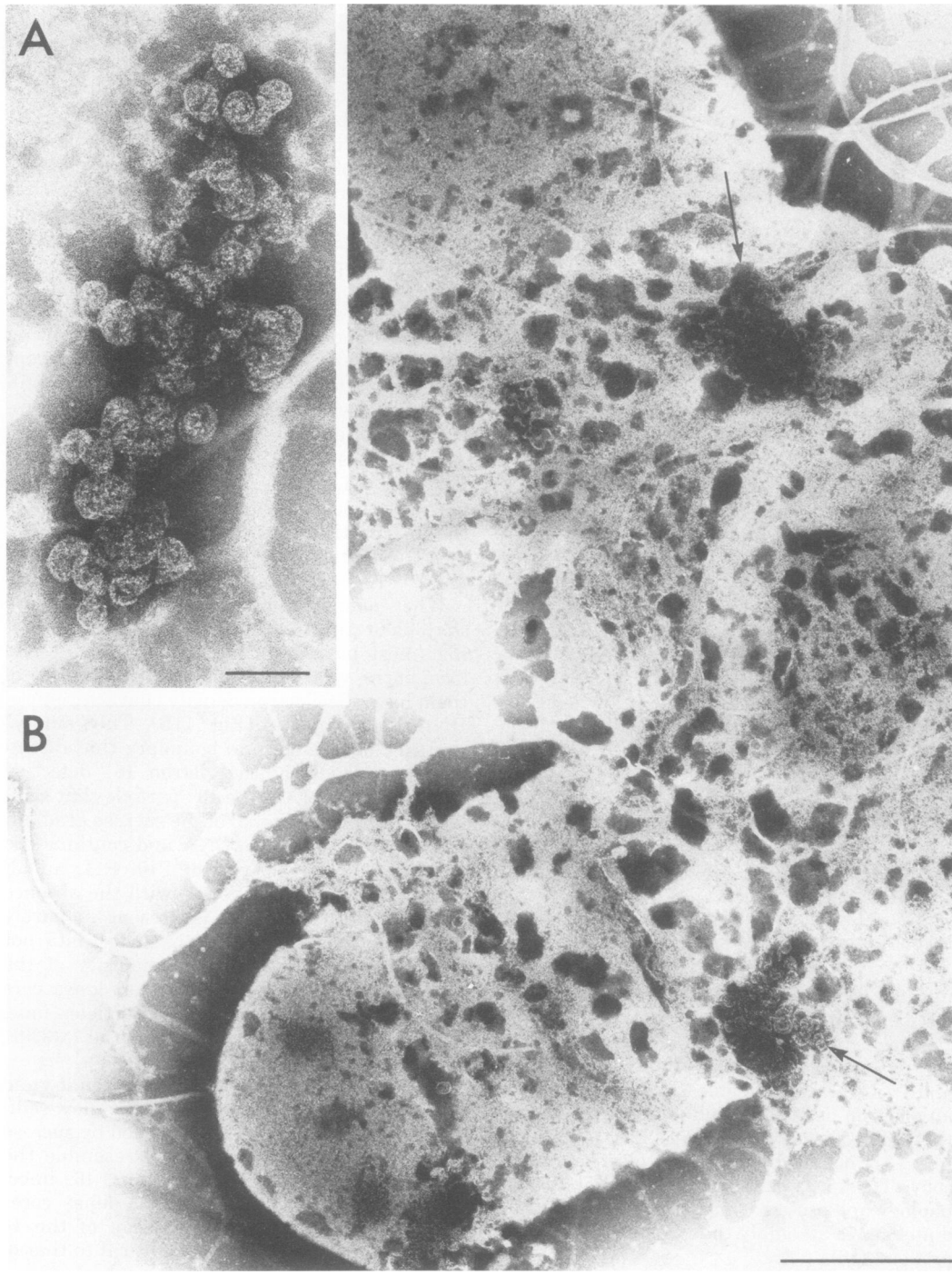

FIG. 7. *Electron micrographs of in situ lysis preparations showing structures with a low degree of organization produced in sus7(701)-infected cells. Arrows indicate clumps of 7⁻ structures. The magnification bars in A and B represent 100 and 500 nm, respectively.*

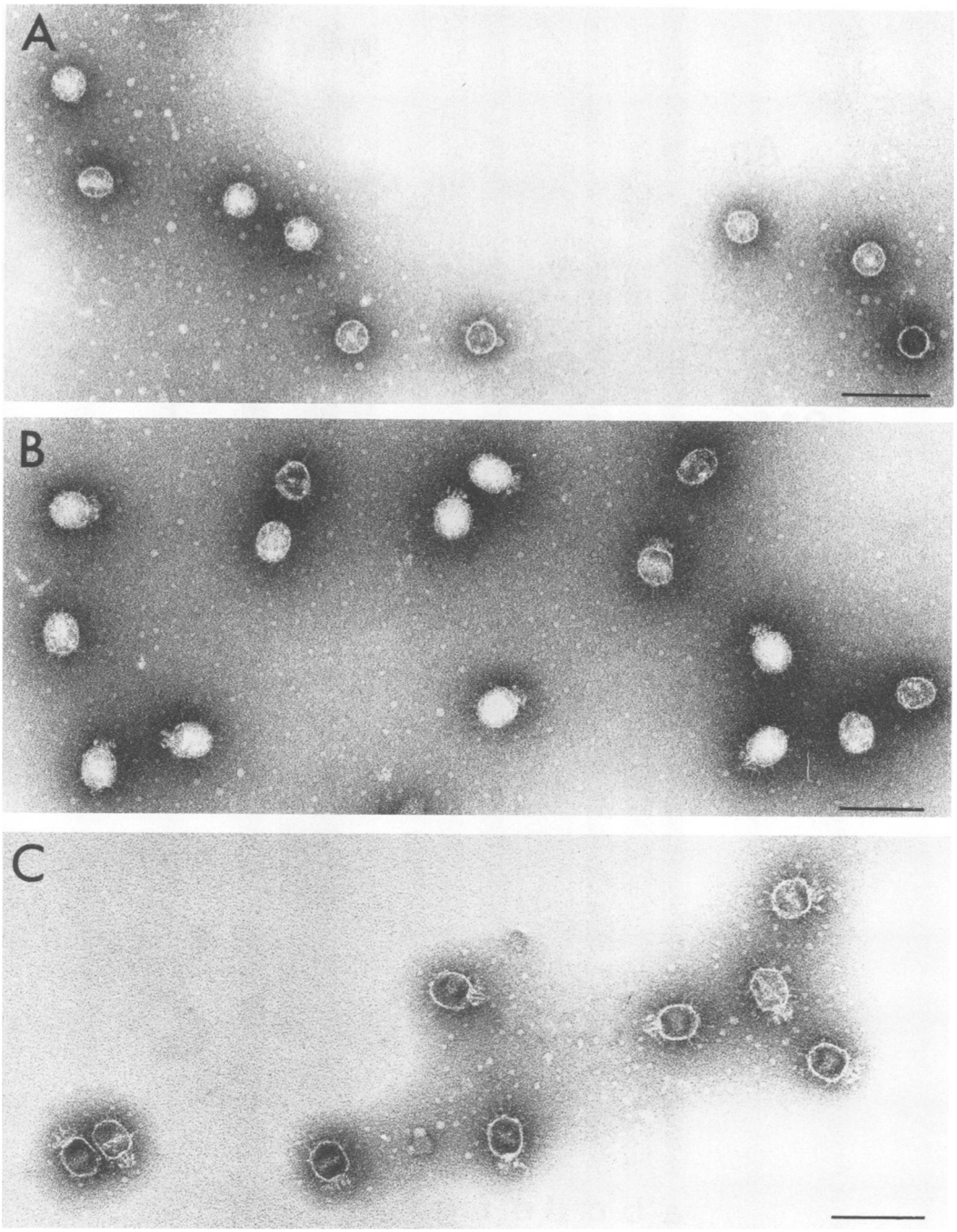

FIG. 8. *Electron micrographs of ϕ29-related structures produced in restrictive sus mutant infections and prepared for microscopy from peak fractions of the sucrose gradients shown in Fig. 5. (A) 10$^-$ isometric heads with electron dense cores; (B) 9$^-$ heads with necks, again showing cores; (C) 13$^-$ heads with necks, but with little core material. Each magnification bar represents 100 nm.*

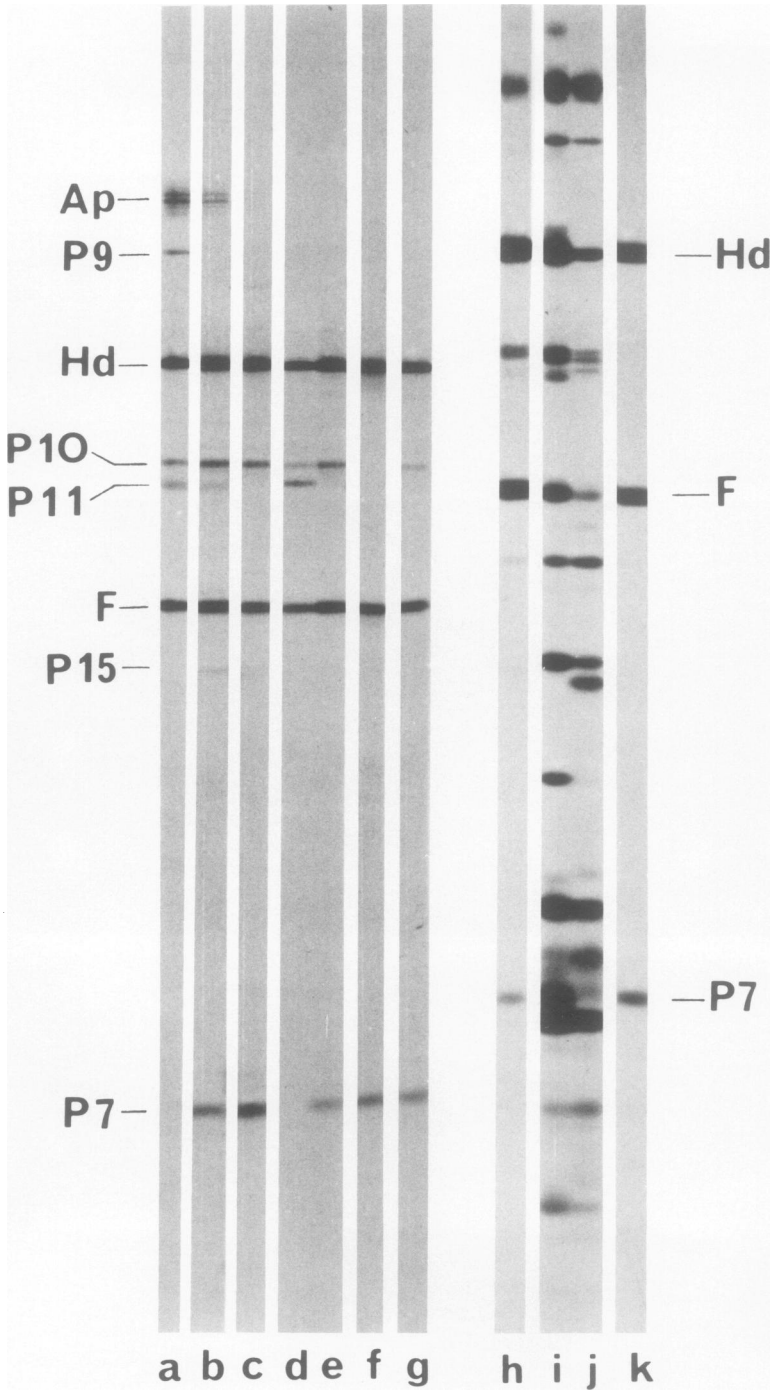

FIG. 9. *Autoradiographs of ^{14}C-labeled φ29 proteins comprising mature φ29 and φ29-related structures produced in restrictive sus mutant infections and isolated by sucrose gradient centrifugation as shown in Fig. 4 and 5. Peak I and/or peak II fractions from the gradients were analyzed for ^{14}C-labeled viral proteins by SDS-polyacrylamide gel electrophoresis followed by autoradiography as described in Materials and Methods. (a) 14$^-$ particles from peak I; (b) 9$^-$ particles; (c) 16$^-$ heads; (d) 11$^-$ heads from peak I; (e) 11$^-$ heads from peak II; (f) 10$^-$ heads; (g) 12$^-$ heads from peak II. The identity of protein P7 was demonstrated by electrophoresis of these same fractions in a slab gel with lysate proteins produced in the wild-type infection. Profiles h and k correspond to those depicted in b and f. Profile i is of a φ29-infected culture supernatant, and profile j is of a φ29-infected cell pellet.*

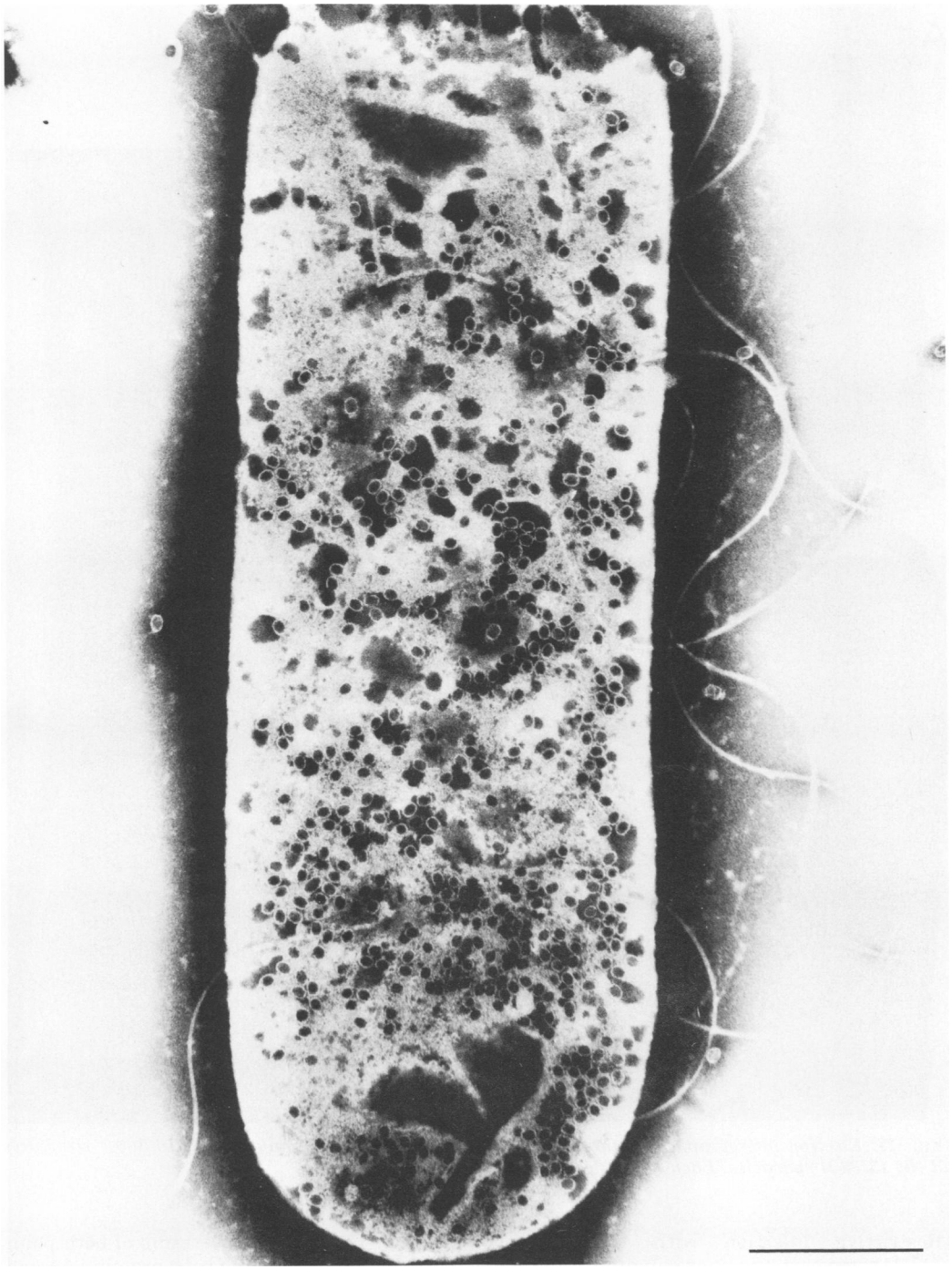

FIG. 10. *In situ lysis preparation of a sus16(300)-infected cell. The magnification bar represents 500 nm.*

that obtained with the 14^- particles (Fig. 4). Peak I contains particles with the morphology and composition of mature ϕ29 (data not shown). Peak II is resolved into two components, each containing the proteins Hd, P10, and F; in addition, the faster-sedimenting particles contain the core protein P7 (data not shown).

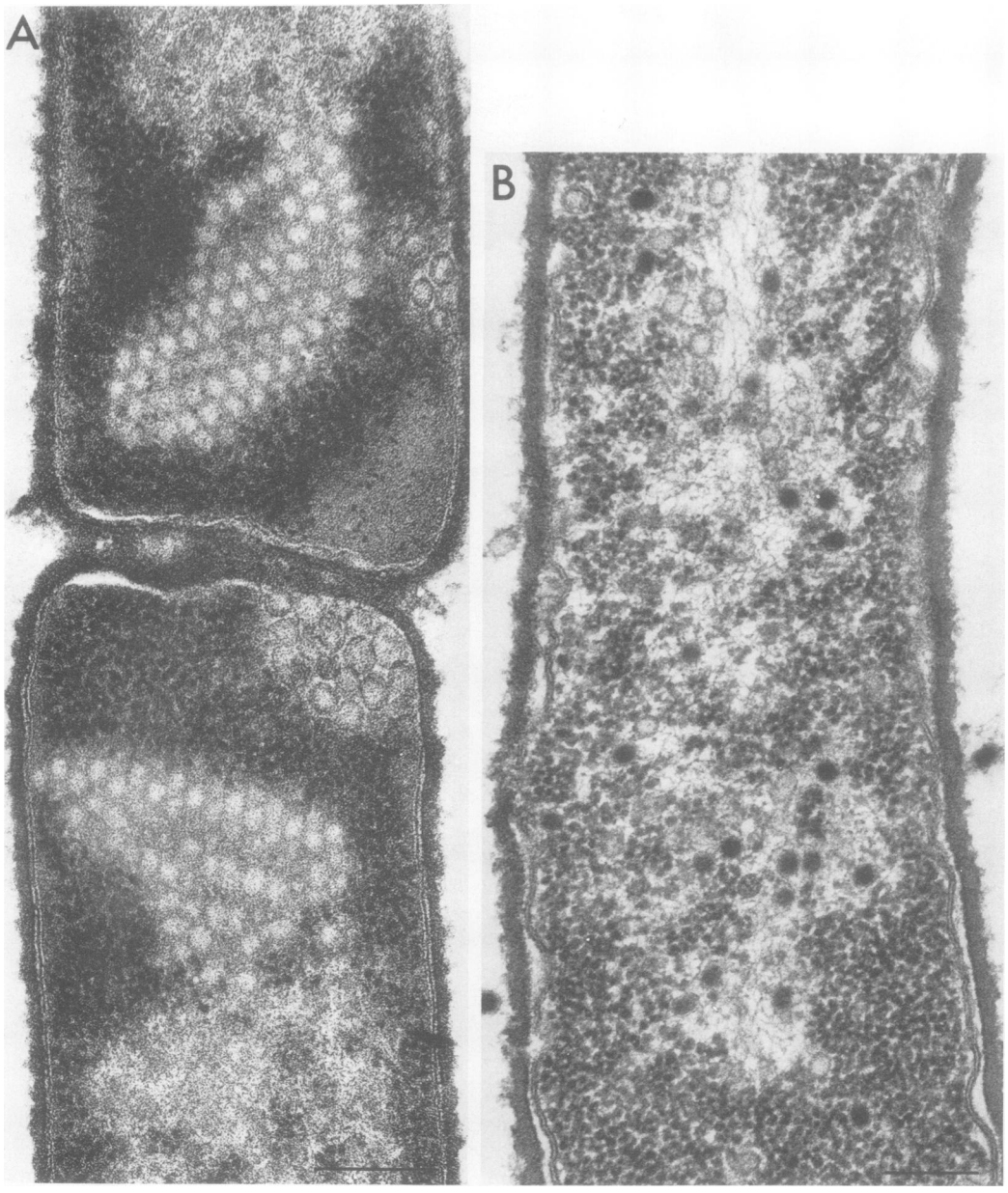

FIG. 11. *Electron micrographs of thin sections of B. subtilis SpoA12 containing (A) 16(300)⁻ structures and (B) 13(330)⁻ particles. Each magnification bar represents 200 nm.*

Restrictive infection with the mutant *sus*17(112) gave a burst approximately half that of wild-type ϕ29, and this mutant could not be placed in cistron 17 by complementation. The phenotype of the mutant *sus*17(741) infection, the inability to synthesize proteins A1 and A2 (2), is the same as that of the *sus*17(112) infection (Fig. 15b and e). Revertants of both point mutations can synthesize both proteins A1 and A2 (Fig. 15a and f).

DISCUSSION

Although our purpose has been to identify cistrons that function during morphogenesis,

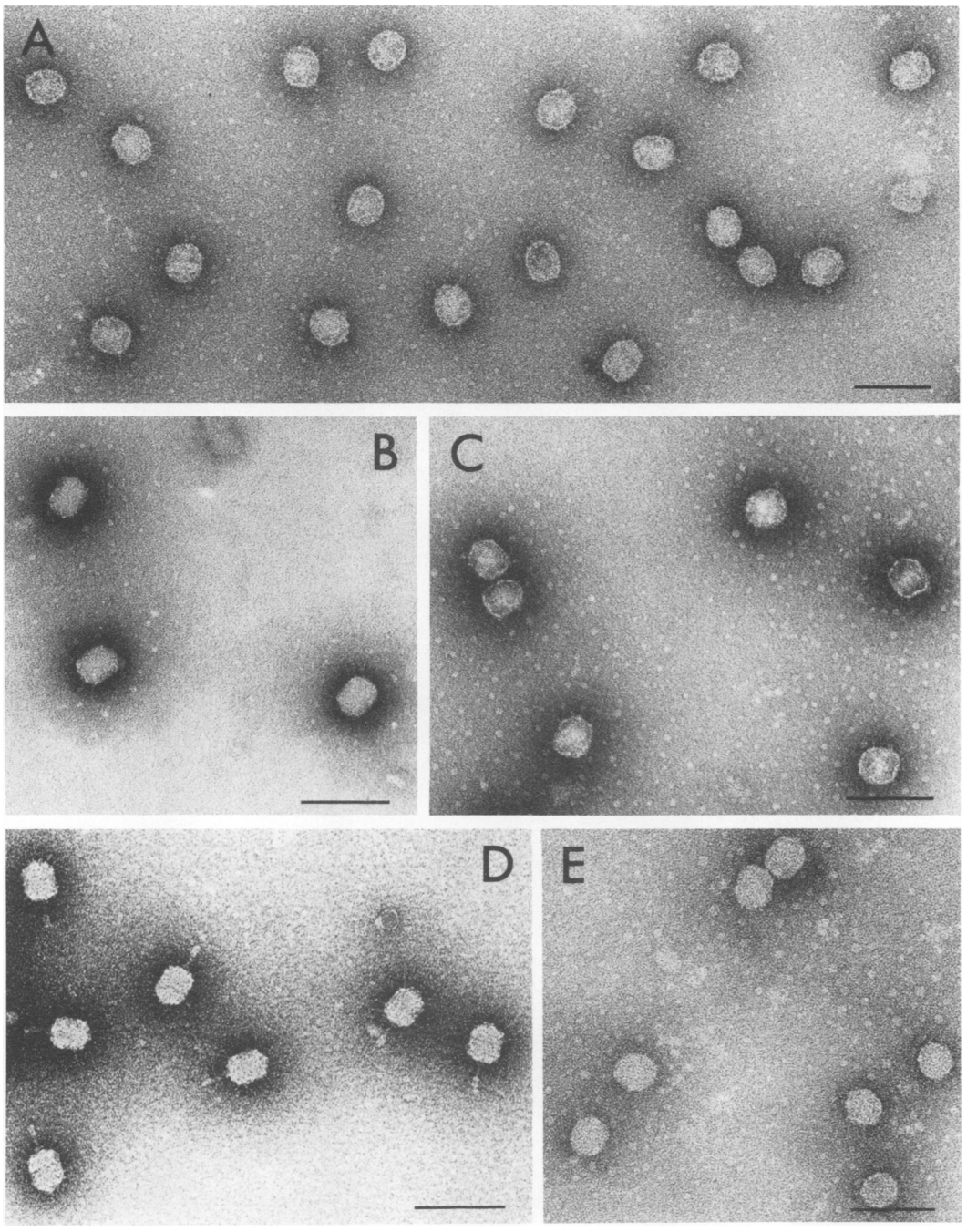

FIG. 12. *Electron micrographs of ϕ29-related structures produced in restrictive sus mutant infections and prepared for microscopy from peak fractions of the sucrose gradients shown in Fig. 4. (A) 16$^-$ heads with electron-dense core material; (B) DNA-containing 11$^-$ heads from peak I; (C) 11$^-$ heads from peak II, some with cores; (D) DNA-containing 12$^-$ particles from peak I; (E) 12$^-$ particles with cores from peak II. Each magnification bar represents 100 nm.*

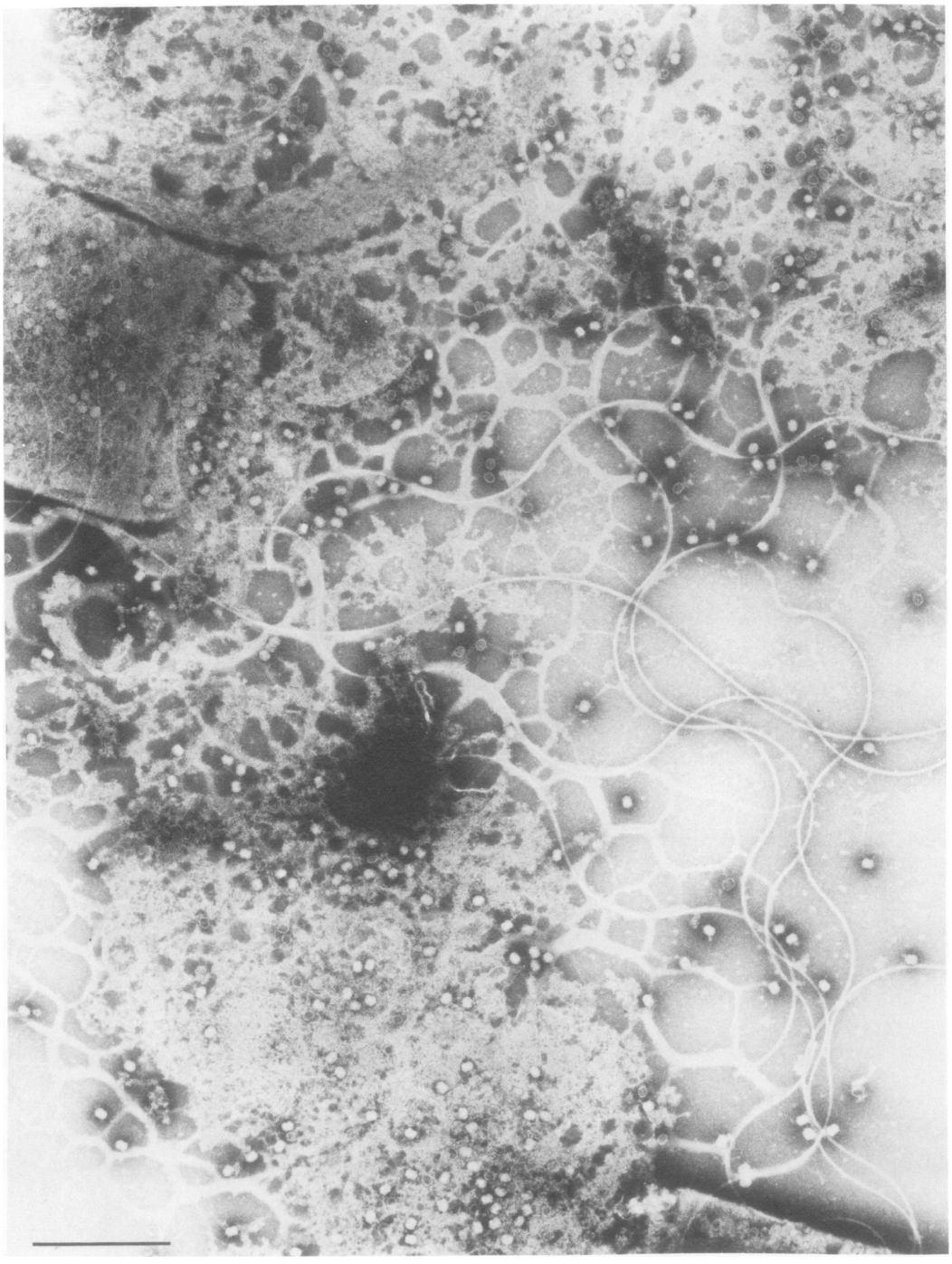

FIG. 13. *In situ lysis preparation of sus11(771)-infected cells. The magnification bar represents 500 nm.*

we have included data to provide a more definitive description of the phenotype of several mutants.

The ϕ29 reference mutants of the Madrid (15) and Minneapolis (20, 21) collections have been used to construct a linear genetic map. Three-factor crosses have been used to determine an unambiguous order for 17 cistrons (Fig. 1; 13).

Viral-specified proteins missing during restrictive infection by mutants of 13 cistrons have been identified (2, 20). The functional clustering of cistrons specifying structural proteins on the ϕ29 genome is summarized in Fig. 2.

The products of cistrons 7, 9, 10, 13, and 16 play an essential role in phage assembly. The nonstructural protein designated LM5B (7) has been shown to be the product of cistron 7, P7 (Fig. 6). In the absence of P7, fragile structures with a low degree of organization can be detected with the in situ lysis technique (Fig. 7). They resemble the phage P22 structures observed in the absence of the gene 8 scaffolding protein (5). All phage-related structures that lack DNA but have an electron-dense core contain P7 (Fig. 9 and Table 1). The protein is an important component of the 16^- particle (Fig. 4 and 9c; Table 1), a particle resembling the "prohead" structure we have shown to be a precursor particle by pulse-chase experiments (16). P7 is absent in any peak I DNA-containing particle resulting from restrictive *sus* mutant infection. This evidence suggests P7 is essential for the formation of any organized and stable head-related structure, and that it must be released prior to or during DNA packaging.

The cistron 16^- head-related structures (Fig. 10 and 12A) lack the normal angularity of the ϕ29 capsid and are composed of the proteins Hd, F, P10, and P7 (Fig. 9 and Table 1). DNA is not packaged in the absence of P16, and the peak II prohead-like structures accumulate. Restrictive infection by mutant *sus*1(629) also results in the accumulation of large numbers of prohead-like particles (Fig. 4 and 14), even though P16 is present. It is possible in this case that viral DNA is not present in the proper "form" to be packaged. Our data indicate that P16 is essential for morphogenesis and suggest that it may function as P7 is replaced by viral DNA.

The isometric particles that form in the cistron 10^- infection (Fig. 8A) contain approximately the same number of copies of the proteins F and P7 in addition to the major head protein (Fig. 9 and Table 1). Prolate, DNA-containing particles have never been observed in 10^- restrictive infection. The neck upper collar protein P10 thus has a dual function. It is a viral component and is essential for the formation of the ϕ29 prolate head.

The peak II particle formed during cistron 9^- restrictive infection (Fig. 5) has the prohead-like morphology and an electron-dense core (Fig. 8B). Many of the particles appear to have neck structures with attached appendages. The protein composition data are in agreement with this observation (Table 1). In the absence of P9, the viral tail protein, stable peak I DNA-containing particles do not form, and thus P9 also has a dual function.

Most cistron 13^- particles observed in thin sections have the angularity of the viral head and the electron density characteristic of DNA-filled particles (Fig. 11B). In contrast, the 13^- particles sediment in peak II of the sucrose gradient (Fig. 5 and 8C), indicating loss of DNA. These observations suggest that DNA packaging may occur in the absence of P13, but that P13 must interact with P9 and P11 to generate the stable mature virion.

We were unable to detect virus-related parti-

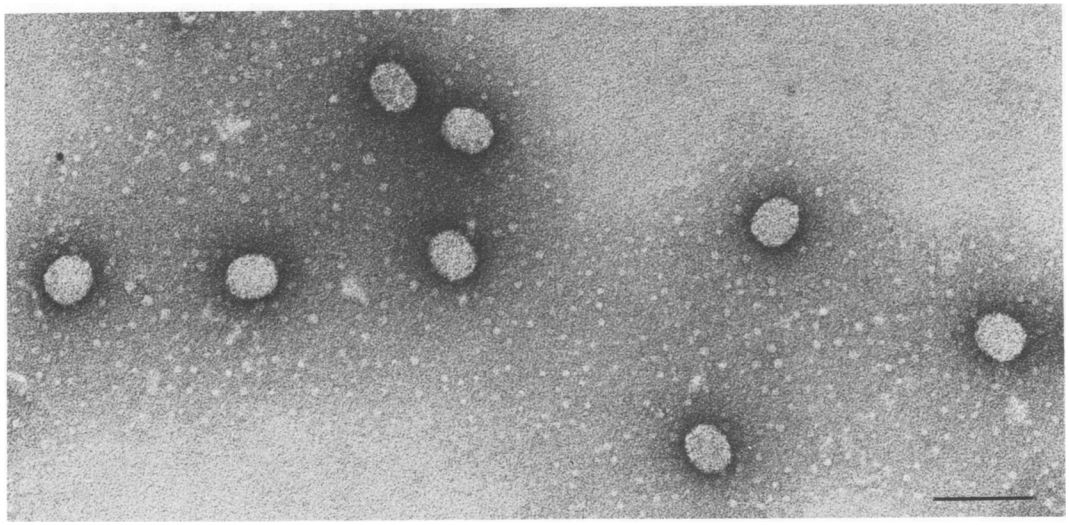

FIG. 14. *Electron micrograph of 1^- particles with cores from peak II, fraction 21, of the sucrose gradient shown in Fig. 4. The magnification bar represents 100 nm.*

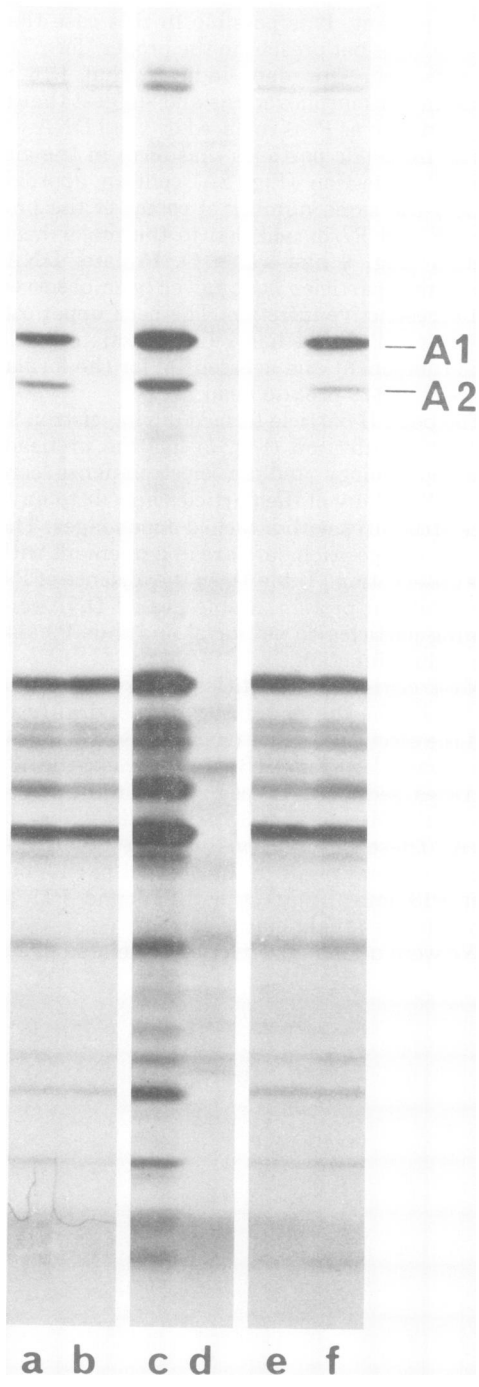

FIG. 15. *Autoradiographs of ^{14}C-labeled φ29-specific early proteins produced in UV-irradiated B. subtilis SpoA12 infected with wild-type φ29, sus mutants, or revertants of sus mutants and analyzed by SDS-gel electrophoresis. Cells were labeled from 2 to 8 min as described in the legend to Fig. 6, and cell pellet fractions were processed for electrophoresis as described in Materials and Methods. (a) sus17(741) revertant; (b) sus17(741); (c) wild-type φ29; (d) uninfected control; (e) sus17(112); (f) sus17(112) revertant.*

cles after infection by mutants of cistrons 2, 3, 4, and 8 by either the thin sectioning or the in situ lysis techniques of electron microscopy. The viral head contains the proteins Hd, P10, and F. Both Hd and F are absent during restrictive infection by mutants of cistrons 4 and 8 (2). Mutants of cistrons 2 and 3 cannot synthesize viral DNA in the nonpermissive host (Fig. 1). P2 may function in the attachment of DNA to the membrane (8; unpublished complementation data). Since viral-induced RNA and protein synthesis occur in the absence of DNA synthesis (7, 10), we might expect to detect the accumulation of prohead-like particles during restrictive infection by cistron 2 and 3 mutants, but we do not. P2 and P3 may ensure that a sufficient number of "DNA-membrane" sites are available to initiate particle assembly, and in this sense may play a dual role during infection.

Viral DNA synthesis is delayed in the *sus*6(626) restrictive infection (Fig. 3B). A few cistron 6$^-$ head structures resembling the 16$^-$ structures shown in Fig. 11A were observed in thin sections of infected cells.

The product of cistron 15, P15, is known, but the function of the protein remains unknown (2). Restrictive infection by *sus*15(212) leads to the production of peak II and peak I particles (Fig. 4) and is characterized by the production of a small burst of infectious particles (data not shown). The only particles known to contain P15 are present in peak II after nonpermissive infection by the mutant *sus*9(756) (Fig. 5, 8B and 9b; Table 1) and sucrose gradient isolation. It is possible that P15 may play a role in assembly.

The cistrons 11$^-$ and 12$^-$ peak I particles contain DNA, and their morphology and composition suggest they may be true intermediates in the assembly process (Fig. 4, 9, 12, and 13; Table 1). The 12$^-$ particle can be converted to viable virus by in vitro complementation (25). These results have led to the hypothesis that the neck and tail are assembled by sequential interaction of P11 and P9 to convert the 11$^-$ particle to the 12$^-$ particle. Cistron 13$^-$ particles lack DNA and frequently have either a complete neck and tail or a neck structure. Thus the unidentified P13 may interact with P9 and P11 to stabilize the completely assembled virion.

Our data sugest that the structural proteins Hd, F, and P10 are essential components of the

prolate "prohead" and that the presence of P7 is required for prohead production. The protein P16 plays an essential role in the conversion of the prohead to structures containing DNA. In the absence of P9 and P10 anomalous particles form, and these particles are probably not intermediates in ϕ29 assembly. All of our evidence is consistent with a single assembly pathway that terminates in the attachment of the appendage protein (25). Other proteins may play a role in the assembly process, but our data on this point are not conclusive.

ACKNOWLEDGMENTS

During the course of this research we have shared mutants and information with M. Salas and E. Vinuela. Our view of ϕ29 assembly results in part from this exchange. We gratefully acknowledge the technical assistance of Charlene Peterson and Viola M. Zeece.

This work was aided by grant GB-29393 from the National Science Foundation and by Public Health Service grants DE-3606 from the National Institute of Dental Research and GM-19743 from the National Institute of General Medical Sciences.

LITERATURE CITED

1. **Anderson, D. L., D. D. Hickman, and B. E. Reilly.** 1966. Structure of *Bacillus subtilis* bacteriophage ϕ29 and the length of ϕ29 deoxyribonucleic acid. J. Bacteriol. 91:2081-2089.
2. **Anderson, D. L., and B. E. Reilly.** 1974. Analysis of bacteriophage ϕ29 gene function: protein synthesis in suppressor-sensitive mutant infection of *Bacillus subtilis*. J. Virol. 13:211-221.
3. **Carrascosa, J. L., A. Camacho, E. Viñuela, and M. Salas.** 1974. A precursor of the neck appendage protein of *B. subtilis* phage ϕ29. FEBS Lett. 44:317-321.
4. **Carrascosa, J. L., E. Viñuela, and M. Salas.** 1973. Proteins induced in *Bacillus subtilis* infected with bacteriophage ϕ29. Virology 56:291-299.
5. **Casjens, S., and J. King.** 1974. P22 morphogenesis. I. Catalytic scaffolding protein in capsid assembly. J. Supramol. Struct. 2:202-224.
6. **Hagen, E. W., and D. L. Anderson.** 1975. In situ lysis of ϕ29- and SPO1-infected *Bacillus subtilis*. J. Virol. 15:217-220.
7. **Hawley, L. A., B. E. Reilly, E. W. Hagen, and D. L. Anderson.** 1973. Viral protein synthesis in bacteriophage ϕ29-infected *Bacillus subtilis*. J. Virol. 12:1149-1159.
8. **Ivarie, R. D., and J. J. Pene.** 1973. DNA replication in bacteriophage ϕ29: the requirement of a viral-specific product for association of ϕ29 DNA with the cell membrane of *Bacillus amyloliquefaciens*. Virology 52:351-362.
9. **Kellenberger, E., and A. Ryter.** 1967. Bacteriology, p. 335-393. *In* B. Siegel (ed.), Modern developments in electron microscopy. Academic Press Inc., New York.
10. **Loskutoff, D. J., J. J. Pene, and D. P. Andrews.** 1973. Gene expression during the development of *Bacillus subtilis* bacteriophage ϕ29. I. Analysis of viral-specific transcription by deoxyribonucleic acid-ribonucleic acid competition hybridization. J. Virol. 11:78-86.
11. **Luft, J. H.** 1961. Improvements in epoxy resin embedding methods. J. Biophys. Biochem. Cytol. 9:409-414.
12. **McGuire, J. C., J. J. Pene, and J. Barrow-Carraway.** 1974. Gene expression during the development of bacteriophage ϕ29. III. Analysis of viral-specific protein synthesis with suppressible mutants. J. Virol. 13:390-398.
13. **Mellado, R. P., F. Moreno, E. Viñuela, M. Salas, B. E. Reilly, and D. L. Anderson.** 1976. Genetic analysis of bacteriophage ϕ29 of *Bacillus subtilis:* integration and mapping of reference mutants of two collections. J. Virol. 19:495-500.
14. **Mendez, E., G. Ramirez, M. Salas, and E. Viñuela.** 1971. Structural proteins of bacteriophage ϕ29. Virology 45:567-576.
15. **Moreno, F., A. Camacho, E. Viñuela, and M. Salas.** 1974. Suppressor-sensitive mutants and genetic map of *Bacillus subtilis* bacteriophage ϕ29. Virology 62:1-16.
16. **Nelson, R. A., B. E. Reilly, and D. L. Anderson.** 1976. Morphogenesis of bacteriophage ϕ29 of *Bacillus subtilis:* preliminary isolation and characterization of intermediate particles of the assembly pathway. J. Virol. 19:518-532.
17. **Ortin, J., C. Vasquez, E. Viñuela, and M. Salas.** 1971. DNA-protein complex in circular DNA from phage ϕ29. Nature (London) New Biol. 234:275-277.
18. **Pene, J. J., P. C. Murr, and J. Barrow-Carraway.** 1973. Synthesis of bacteriophage ϕ29 proteins in *Bacillus subtilis*. J. Virol. 12:61-67.
19. **Reilly, B. E., and J. Spizizen.** 1965. Bacteriophage deoxyribonucleate infection of competent *Bacillus subtilis*. J. Bacteriol. 89:782-790.
20. **Reilly, B. E., M. E. Tosi, and D. L. Anderson.** 1975. Genetic analysis of bacteriophage ϕ29 of *Bacillus subtilis:* mapping of the cistrons coding for structural proteins. J. Virol. 16:1010-1016.
21. **Reilly, B. E., V. M. Zeece, and D. L. Anderson.** 1973. A genetic study of suppressor-sensitive mutants of the *Bacillus subtilis* bacteriophage ϕ29. J. Virol. 11:756-760.
22. **Reynolds, E. A.** 1963. Lead citrate staining technique. J. Cell. Biol. 17:208-211.
23. **Schachtele, C. F., B. E. Reilly, C. V. DeSain, M. O. Whittington, and D. L. Anderson.** 1973. Selective replication of bacteriophage ϕ29 deoxyribonucleic acid in 6-(*p*-hydroxyphenylazo)-uracil-treated *Bacillus subtilis*. J. Virol. 11:153-155.
24. **Tosi, M., and D. L. Anderson.** 1973. Antigenic properties of bacteriophage ϕ29 structural proteins. J. Virol. 12:1548-1559.
25. **Tosi, M. E., B. E. Reilly, and D. L. Anderson.** 1975. Morphogenesis of bacteriophage ϕ29 of *Bacillus subtilis:* cleavage and assembly of the neck appendage protein. J. Virol. 16:1282-1295.